




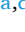








Fass and C3/C4 contribute to the activities and levels of the protein phosphatase 2A catalytic subunit pool and regulate mitotic events in Arabidopsis

Adrienn Kelemen^{a,1} , Zoltán Kónya^{b,1} , László Ujlaky-Nagy^c , Tamás Garda^a , Ferenc Erdódi^b , Csongor Freytag^{a,d} , Gabriella Petra Juhász^a , Taras P. Pasternak^e , Milán Riba^a , Csaba Máthé^{a,*} 

^a Plant Cell and Developmental Biology Research Group, Department of Botany, Faculty of Science and Technology, University of Debrecen, Egyetem Ter 1, Debrecen, H-4032, Hungary

^b Department of Medical Chemistry, Faculty of Medicine, University of Debrecen, Egyetem Ter 1, Debrecen, H-4032, Hungary

^c Department of Biophysics and Cell Biology, Faculty of Medicine, University of Debrecen, Egyetem Ter 1, Debrecen, H-4032, Hungary

^d "One Health" Institute, Faculty of Health Science, University of Debrecen, Nagyerdei Blvd. 98, H-4032, Debrecen, Hungary

^e Instituto de Bioingeniería, Universidad Miguel Hernández, 03202 Elche, Spain

ARTICLE INFO

Handling Editor: Ying HUANG Zhen-

Keywords:

Protein phosphatase

PP2A

C3-C4 subunits

Fass- B" subunit

Mitosis

Histone H3 phosphorylation

Microcystin-LR

ABSTRACT

The serine-threonine protein phosphatase PP2A holoenzymes regulate many eukaryotic cellular processes. They consist of catalytic (C), regulatory (B) and scaffolding (A) subunits. C3-C4 and their interacting B" (Fass) subunits of PP2A were in the focus of this study. Our tools were Arabidopsis wild-type plants and phosphatase mutants-*fass* (B"), *c3c4* and microcystin-LR (MCY-LR), a specific inhibitor of PP2A/PP1. We have studied their role in the regulation of protein phosphatase activities and expression. In relation to this, we have focused on their involvement in mitotic activity and histone H3 phosphorylation.

We show here for the first time that besides C3-C4, B"/Fass subunit has a crucial role in the maintenance of normal protein phosphatase activities and levels in Arabidopsis. *fass* mutants show increased activities of PP2A and PP1 (a phosphatase related to PP2A) and increased expression of PP2A/C. Both overall PP2A and PP1 activities are inhibited in *c3c4*. Fass and C3-C4 are involved in the regulation of mitotic activity. C3-C4 have less direct influence on the onset of mitosis, but Fass is involved in the regulation of metaphase-anaphase transition. In wild-type plants, MCY-LR inhibited PP2A/C activities, related to alterations of mitotic events. Distinct effects of MCY-LR in mutants also reveal the role of Fass/C3-C4 in the biochemical functionality of PP2A. Fass and C3-C4 regulate the phosphorylation of histone H3, but this effect is not related to the regulation of mitotic onset in Arabidopsis. This study gives new insights into the regulatory roles of Fass and C3-C4 subunits during mitosis in plants.

1. Introduction

One of the key eukaryotic cellular regulatory processes is reversible protein phosphorylation of which the non-metal dependent serine-threonine protein phosphatases PP2A and PP1 are major players (Shi, 2009). PP2A holoenzyme consists of three subunits, the catalytic (C) subunit with five isoforms in Arabidopsis, the variable scaffolding (A)

and highly variable regulatory (B) subunits with multiple (B, B', B", B''') subfamilies (Bheri and Pandey, 2019; Farkas et al., 2007). PP1 bears the catalytic (C) subunits bound to stimulatory or inhibitory regulator (R) proteins and it also has multiple variants (up to nine PP1C isoforms in Arabidopsis, Farkas et al., 2007). The variable regulatory subunits of both phosphatase types are responsible for the diverse subcellular localization and substrate specificity of holoenzymes (Shi, 2009;

* Corresponding author.

E-mail addresses: keleadri0613@gmail.com (A. Kelemen), konya.zoltan@med.unideb.hu (Z. Kónya), lnagy@med.unideb.hu (L. Ujlaky-Nagy), gtamas0516@gmail.com (T. Garda), erdodi@med.unideb.hu (F. Erdódi), freytagcsongor@gmail.com (C. Freytag), juhaszgabriellapetra@gmail.com (G.P. Juhász), taras.p.pasternak@gmail.com (T.P. Pasternak), milan.riba@gmail.com (M. Riba), mathe.csaba@science.unideb.hu (C. Máthé).

¹ Contributed equally.

<https://doi.org/10.1016/j.plaphy.2025.110187>

Received 10 December 2024; Received in revised form 10 May 2025; Accepted 21 June 2025

Available online 21 June 2025

0981-9428/© 2025 The Authors.

Published by Elsevier Masson SAS. This is an open access article under the CC BY-NC-ND license

(<http://creativecommons.org/licenses/by-nc-nd/4.0/>).

Virshup and Shenolikar, 2009).

Fass (TONNEAU2) is a type B" regulatory subunit of PP2A, involved in several key subcellular events including microtubule organization in non-dividing and dividing plant cells (Camilleri et al., 2002; Kirik et al., 2012; Spinner et al., 2013). It is part of the TTP complex, together with TRM (TON1 Recruiting Motif) necessary for assembly and targeting of the complex and TON1 as a regulator and the PP2A holoenzyme (Motta and Schnittger, 2021; Schaefer et al., 2017; Spinner et al., 2013). The connection between TRM and Fass is thought to be important for the proper subcellular targeting of the PP2A holoenzyme-in particular, to microtubules (MTs) to exert the regulatory role of TTP in MT organization (Rasmussen and Bellinger, 2018; Spinner et al., 2013). Fass is known to interact with the C3 and C4, class II catalytic subunits of PP2A with similar functions (Camilleri et al., 2002; Spinner et al., 2013). These two subunits have redundant functions in the control of embryo patterning and proper root development (Ballesteros et al., 2013). Concerning the overall activities and expression of PP2A catalytic subunits (PP2A/C), the contribution of Fass subunits is less understood.

One of the key functions of reversible protein phosphorylation is cell cycle and particularly, mitotic regulation. Regarding the relevant role of protein phosphatases, although several new findings are available for all eukaryotic cells including plants, there is still less knowledge in this field as compared to phosphorylation catalyzed by protein kinases. Concerning the Fass and C3-C4 subunits of PP2A, they are known to regulate mitosis via influencing MT assembly during early stages (Schaefer et al., 2017; Spinner et al., 2013). However, much research should be performed in order to find more mechanistic details e.g. on how Fass (and C3-C4) influence protein phosphatase functionality both at the whole-plant level and during plant mitosis and how all these subunits influence mitotic structures or post-translational modifications of key protein players.

In plants, phosphorylation of histone H3 at the Ser10 position is characteristic only for mitotic cells. In general, phosphorylation is mediated by Aurora kinases, e.g. AtAurora1 (see Demidov et al., 2005 for an example). The inhibition of protein phosphatase activities increases the level of H3 phosphorylation in plants like broad bean/*Vicia faba* (Beyer et al., 2012). Normally, the formation of Ser10 phosphorylated histone H3 (pH3-Ser10) starts at early prophase at the pericentromeric region of chromosomes, playing a role in the mediation of mitotic chromatin condensation. The maximum rate of H3 phosphorylation is reached in metaphase, where pHSer10 is present not only around centromeres, but in chromosome arms as well. At metaphase-anaphase transition, the levels of pH3 decrease to allow sister chromatid segregation. This decrease continues in late mitosis in parallel with the relaxation of mitotic chromatin and in late cytokinesis will be hardly detectable (Beyer et al., 2012; Houben et al., 2007). To date, there are no data on whether B" and C3-C4 subunits of PP2A influence dephosphorylation of pH3-Ser10 during plant mitosis in relation to overall PP2A/C activities and levels. There is research work suggesting involvement of PP1 (see Discussion section).

We used wild-type seedlings and the *fass-5* (strongly altered phenotype), *fass-15* (phenotype is altered at a lesser grade) mutants as well as the *c3c4* double mutants of Arabidopsis described by Alonso et al. (2003), Camilleri et al. (2002), Kirik et al. (2012); Spinner et al. (2013). *fass-5* is strongly altered in both shoot and root development, while *fass-15* and *c3c4* are stunted, but show axial organs and develop flowers and *c3c4* has offspring. As such, they are used for the study of subcellular functions of these subunits (Spinner et al., 2013).

Microcystin-LR (MCY-LR) is a cyanobacterial heptapeptide, a specific and potent inhibitor of both PP2A and PP1. Due to its high specificity, it proved to be an excellent tool for the study of regulation of plant subcellular processes by protein phosphatases (Máthé et al., 2016, 2021). We have used it as a research tool in the present study to place our findings on Fass and C3-C4 in the general context of protein phosphatases: for many organisms, it inhibits all isoforms of PP2A and PP1 catalytic subunits (MacKintosh and Diplexcito, 2010).

Besides their role in the localization and substrate specificity of PP2A, several "B" subunits are modulating the activity of the holoenzyme (Máthé et al., 2023). Our central hypothesis was that Fass subunits are doing so, although there were nearly no previous data on this. Thus, an additional mechanism of mitotic regulation by Fass (through the interacting C3/C4 subunits) would be their activity modulatory function for controlling phosphorylation state of cell cycle regulatory proteins including that of histone H3.

In the light of the above statements, the aims of the present study are as follows.

- (i) To reveal the contributions of Fass and their interacting C3-C4 subunits of PP2A holoenzyme to the overall protein phosphatase functionality/activities and expression of the total catalytic subunit pool.
- (ii) To reveal their role played in the proper mitotic activity and the onset of mitosis in the Arabidopsis root apical meristem (RAM). Related to this, to reveal their role in the regulation of histone H3 phosphorylation during mitosis. All these aspects were aimed to be studied in relation to the above mentioned overall PP2A functionalities and expression.

2. Materials and methods

2.1. Plant material and MCY-LR treatments

The genotypes of *Arabidopsis thaliana* used in this study were (i) wild-type Columbia ecotype (Col0) (ii) the protein phosphatase (PP2A) related mutants described by Alonso et al. (2003), Camilleri et al. (2002), Kirik et al. (2012) and Spinner et al. (2013): *c3c4*, a double T-DNA insertion mutant for the respective catalytic subunits and the *fass* (*ton2*) mutants for the B" regulatory subunit. The *fass-15* and *fass-5* loss-of-function mutants used were created by EMS mutagenesis. They are characterized by abnormal phenotypes with *fass-5* as a strongly altered phenotype with the lack of fully differentiated axial organs (Spinner et al., 2013). These well visible developmental anomalies are present only for the homozygote recessive (HZ) genotypes used throughout our experiments.

Seed sterilization, seedling culture and the method for drug treatments were performed essentially according to Freytag et al. (2021) and Nagy et al. (2018). Surface sterilized seeds were transferred to Murashige-Skoog medium with Gamborg's vitamins (Gamborg et al., 1968; Murashige and Skoog, 1962). After a 48 h-cold treatment, plates with seeds were transferred to a plant tissue culture chamber under a 14/10 h photoperiod, 22 ± 2 °C, $60 \mu\text{mol m}^{-2}\text{s}^{-1}$ photon flux density in the light period. Five days after, seedlings were transferred on sterilized filter paper soaked in liquid modified MS media and treatments (0.05 and 1 μM microcystin-LR/MCY-LR) started. High quality (≥ 95 % purity) MCY-LR used in this study was purified in our laboratories as described previously (Kós et al., 1995, modified by Vasas et al., 2004). Pooled cyanobacterial (*Microcystis aeruginosa* BGSD243) cells were extracted with methanol, followed by removal of the organic solvent and resuspension of dried samples in Tris-HCl, pH 7.5. These aqueous suspensions were subjected to ion-exchange (DEAE-cellulose), then size exclusion (Toyopearl) chromatography. Purity of preparations was checked by an HPLC method (see Freytag et al., 2021).

The concentrations of MCY-LR were carefully selected after preliminary assays for the effects of the inhibitor. Therefore, we avoided high concentrations (above 2 μM) that proved to be lethal or severely harmful for plants in a short term. Treatments lasted for 24 h for each type of experiments presented in this study.

2.2. The assay of protein phosphatase activities and expression

For Col0, phosphatase activities were measured both in whole seedlings and in whole roots of seedlings. For *fass-5* HZs, *fass-15* HZs and

c3c4, roots were frequently not distinguishable (for *fass-5*, the stronger *fass* phenotype) and/or we could not collect enough root material for the assays, thus for these genotypes (along with Col0 seedlings for a reference) we measured activities from whole seedlings.

Protein phosphatase assays were performed essentially as described previously (Erdódi et al., 1995; Garda et al., 2018; Máthé et al., 2013). Briefly, plant extracts were prepared with 50 mM Tris-HCl (pH 7.5), 0.1 mM EDTA, 0.2 mM EGTA, 0.1 % (w/v) DTT, 0.2 mM PMSF (Sigma-Aldrich, St. Louis, MO., USA) and 0.5 % (v/v) protease inhibitor cocktail (Roche Appl. Sci., Indianapolis, IN, USA). After centrifugation, protein content of supernatants was assayed according to Bradford (1976). The substrate for the phosphatase assay was ^{32}P -MLC20 (turkey gizzard 20 kDa myosin light chain). Specific protein phosphatase activities were expressed as pmol ^{32}P i released mg protein $^{-1}$. To distinguish PP2A and PP1 activities, 2 μM Inhibitor-2 (I-2) protein was used (Dedinszki et al., 2015). Total (PP2A + PP1) as well as PP2A and PP1 activities were all measured in 3–6 repetitions for each plant sample.

For the assay of PP2A catalytic (PP2A/C) subunit levels, Western blot analyses of protein extracts from whole seedlings were performed by using the methods of Freytag et al. (2023); Waadt et al. (2008), further modified in our laboratory. Seedlings were homogenized in a buffer containing 50 mM Tris-HCl, pH 7.5, 0.1 mM EDTA, 0.2 mM EGTA, 1 mM phenyl methyl sulphonyl fluoride (PMSF, PanReac AppliChem, Darmstadt, Germany), 2x protease inhibitor cocktail, β -mercaptoethanol (Sigma-Aldrich), 4 % (w/v) poly-vinyl-pyrrolidone (PVP). Extracts were then centrifuged at 20,000 \times g for 20 min (Beckman Avanti series centrifuge, Beckman, Indianapolis, IN, USA) at 4 °C. Protein content of supernatants was assayed by the Bradford (1976) method, then Laemmli buffer was added and samples were subjected to boiling at 95 °C for 5 min. Equal amounts of proteins (10 μg) were loaded on gels, along with a molecular weight marker (Thermo Fisher Scientific, Waltham, MA., USA). Running gel contained 12 % (w/v) polyacrylamide. SDS-PAGE was according to Laemmli (1970). Proteins were blotted into nitrocellulose membranes (Millipore, Burlington, Ma., USA) with an electroblot system (Cleaver Scientific, Rugby, UK). The transfer buffer was 25 mM Tris; 192 mM glycine; 20 % (v/v) methanol; pH 8.3. Membranes were then blocked with 1xTBST (1xTBS + 0,05 % Tween 20) + 5 % (w/v) BSA for 1 h at room temperature. Afterwards, primary antibodies were applied. Polyclonal anti-PP2A/C raised in rabbit (Sigma-Aldrich) was used at a dilution (in TBST + 3 % BSA) of 1:3000, while anti- β -tubulin (Abcam, Cambridge, UK) was used as a loading control at a dilution of 1:12000. Labeling was performed overnight at 4 °C. After several washing steps, a HRP conjugated goat anti-rabbit secondary antibody (Abcam) was applied at a 1:4000 dilution for 2 h at room temperature. After several washing steps, protein bands were detected by the Chemidoc Touch chemoluminescence system (BioRad, Hercules, CA., USA). At least thirty seedlings per treatment per experiment were used and at least three independent experiments were performed. Bands were quantified with the GelAnalyzer19.1® software (Lazar and Lazar) and expressed as pixel numbers. Values for PP2A/C bands were normalized to β -tubulin and plotted.

2.3. Immunohistochemistry and histochemistry. The quantification of mitotic activities

Mitotic figures were detected essentially by labeling of MTs (immunohistochemistry) and chromatin (DAPI staining). However, prophase are not well distinguishable solely by these methods in Arabidopsis. Since labeling of Ser10-phosphorylated histone H3 by immunohistochemistry is ideal for detecting prophase (Beyer et al., 2012 and this study), this method was employed together with MT and DAPI labeling.

Immunohistochemistry methods used in principle the whole mount labeling protocols for Arabidopsis roots as described previously (Freytag et al., 2021; Pasternak et al., 2015). Briefly, intact tips of control and MCY-LR treated primary roots were fixed with 2 % (w/v)

paraformaldehyde (PFA) + 0.1 % (v/v) Triton X-100 in 2x microtubule stabilizing buffer (MTSB). Vacuum infiltration was performed twice for 5 min, then further incubation occurred for 50 min without vacuum; then samples were washed with 1x MTSB three times. Root tips were treated with methanol and rehydrated with a series of decreasing methanol concentrations. Afterwards, cell walls were digested with 0.2 % (w/v) Driselase (Sigma-Aldrich) and 0.15 % macerozyme (Serva Electrophoresis GmbH, Heidelberg, Germany) in 2 mM MES (Sigma-Aldrich) for 25 min at 37 °C and samples were washed with 1x MTSB. Seedlings were then permeabilized with 10 % (v/v) DMSO/3 % (v/v) IGEPAL (Sigma-Aldrich) in 1x MTSB for 20 min at 37 °C and washed with 1x MTSB. Samples were pre-incubated in 1x MTSB + 4 % (w/v) BSA (Sigma-Aldrich) for 30 min. For obtaining higher resolution mitotic cytoskeletal figures (for checking purposes/without pH3-Ser10 labeling, see Suppl. Fig. 1a), samples were incubated with primary anti- β -tubulin antibody in 1x MTSB + 4 % BSA overnight at 4 °C, then washed with 1x MTSB. The primary antibody was anti- β -tubulin raised in rabbit (Abcam) at a 1:100 dilution. Secondary antibody was Alexa 488 conjugated anti-rabbit IgG generated in goat (Abcam) diluted 1:200. Incubation with secondary antibody was in 1x MTSB + 4 % BSA for 4h at 37 °C, then samples were washed with 1x MTSB and counterstained with 3 $\mu\text{g mL}^{-1}$ 4',6'-diamidino-2-phenylindole (DAPI, Fluka, Buchs, Switzerland) to visualize all nuclei according to Beyer et al. (2012). Preparations were analyzed with a Zeiss LSM 880 (Carl Zeiss AG, Jena, Germany) confocal microscope with Zen Black 2.3 software and the conventional settings for Alexa 488 visualization (Arg laser for excitation; emission was observed beside a 490 nm dichroic mirror and a 490–530 filter set). DAPI visualization was performed with a 405 nm diode laser and signal detection was as for the conventional LSM parameters for this dye.

The antibodies used for pH3-Ser10 labeling were: anti-Ser10 phospho-histone H3 diluted 1:50 (primary antibody, Abcam) and Alexa 488 conjugated rabbit polyclonal secondary antibody (IgG) (Abcam) diluted 1:100. Labeling protocol was essentially the same as described above.

For pH3-Ser10 labeling and DAPI counterstaining, microscopy parameters were as follows. Samples were immediately visualized with a Nikon Ti-E inverted super-resolution microscope (Nikon Instruments Inc., Melville, NY, USA) with NIS-elements Ar software (version number: 5.30.02). We used Plan Apo VC 60x A WI DIC N2 objective. For DAPI dye visualization we used 405 nm laser (Excitation/Emission wavelength 405/450), and for the detection of Alexa 488 dye we used 488 nm laser (Excitation/Emission wavelength 488/550).

For the proper detection of mitotic figures, labeling of pH3-Ser, of β -tubulin and chromatin were performed altogether. In this case, a direct labeling method for β -tubulin labeling was more suitable, thus a 50-fold diluted Cy3-conjugated anti- β -tubulin antibody (Sigma-Aldrich) was used simultaneously with the anti-pH3-Ser10 primary antibody (see above). This was followed by the use of the Alexa488 rabbit secondary antibody and DAPI staining (see above). Cy3 was detected by a 561 nm laser on the Nikon CLSM, while Alexa 488 and DAPI was detected as described above.

2.4. The quantification of mitotic activities and histone H3 phosphorylation signal

Mitotic indices were calculated as the percentage of total mitotic as well as early (prophase + prometaphase + metaphase, P + PM + Me) and late (anaphase + telophase + cytokinesis, A + T) mitotic cells out of the total cell number of RAMs from primary roots. The quiescent center (QC) zone and the meristematic cells that will give rise to vascular tissue and root cap region were excluded from counting. Roots of at least three seedlings per treatment per experiment were used and at least five independent experiments were performed.

Quantification of pH3-Ser10 labeling intensity was performed with the aid of the Fiji (ImageJ for Win64) software (Linkert et al., 2010; Schindelin et al., 2012) and given as number of pixels showing area

integrated optical density/AIOD after background extraction. Roots of at least three seedlings per treatment per experiment were used and at least five independent experiments were performed.

2.5. Data analysis

All quantified data were plotted –plots are showing the mean \pm SE values-with the aid of Systat Sigma Plot 10.0[®] and 12.0[®] softwares (Systat Software, San Jose, CA). “X” symbols on graphs = significant differences between control wild-type (Col0) and control mutants, “*” symbols = significant differences between treatments within a given genotype. Statistical significances for the differences between controls and treatments were studied by a post-hoc: Holm-Sidak method and t-tests. Symbols for significant differences on the graphs: X, * = significant difference ($P < 0.05$), XX, ** = significant difference ($P < 0.01$), XXX, *** = significant difference ($P < 0.001$). For more clarity, important changes were labeled with numbers on graphs.

3. Results

3.1. *Fass* and *C3-C4* modulate both PP2A/PP1 activities and PP2A catalytic subunit expression

Concerning the genotypes involved in the present study, both untreated and MCY-LR treated seedlings were analyzed.

Protein phosphatase activity assays of whole seedlings showed that for both the *fass-15* and *fass-5* homozygote mutants (not MCY-LR treated), total PP2A + PP1 activities were higher than in Col0 and this increase was significant for *fass-5* (Fig. 1a, upper chart). Middle and lower charts of Fig. 1a show that increases of both PP2A only and PP1 only activities (assayed separately) accounted for this. For the *c3c4* mutant, there were significant decreases of not only total and PP2A, but of PP1 activities as well (Fig. 1a, all charts).

In the wild-type (Col0) genotype, total (PP2A + PP1) as well as PP2A activities were inhibited significantly in a similar manner by 1 μ M MCY-LR in roots (Fig. 2b, number 3 on graphs) and whole seedlings (Fig. 2a, number 1 on graphs). Meanwhile, PP2A was inhibited significantly by 0.05 μ M MCY-LR in roots (Fig. 2b, middle graph, number 3), but not the whole seedlings (Fig. 2a), where most of fresh weight is given by the shoot system. PP1 was not affected significantly by MCY-LR in any of the

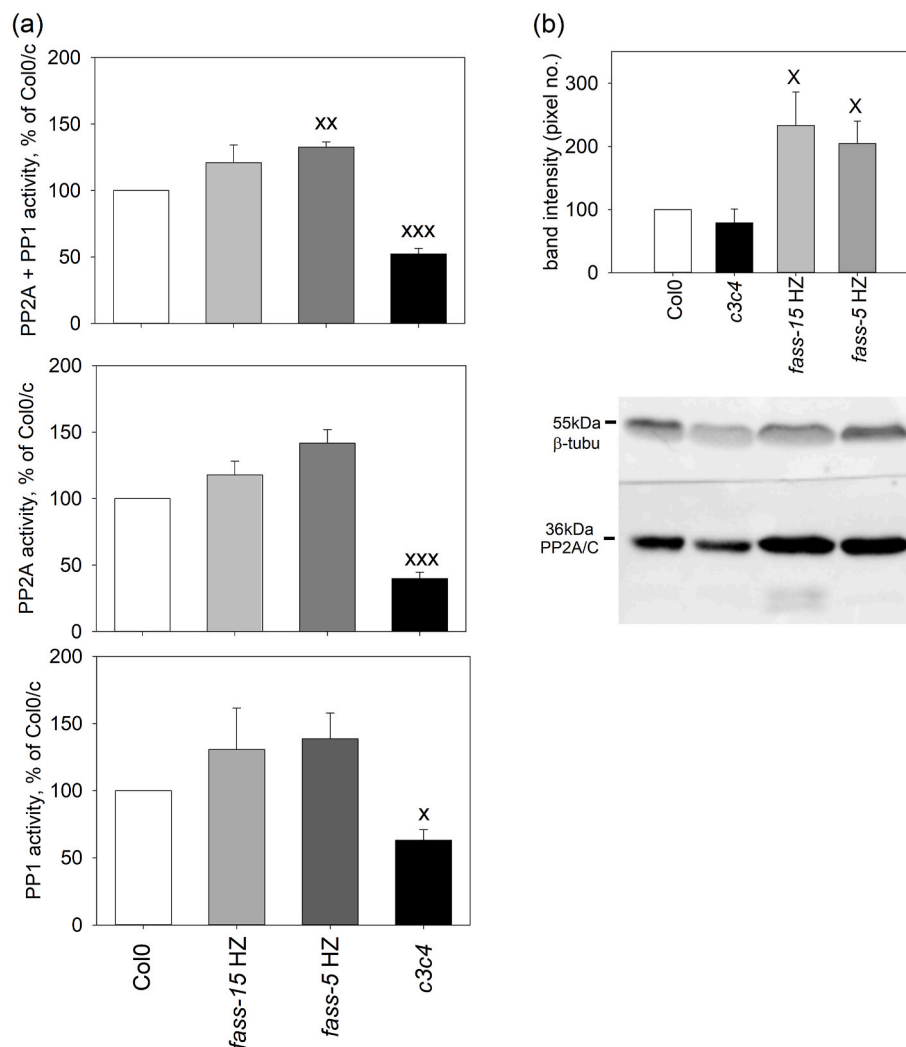


Fig. 1. (a) Protein phosphatase activities for the controls of all genotypes involved in this study show that the *fass* mutations (homozygotes, HZs) increase and not decrease PP2A (and PP1) activities, while decreases are observed for *c3c4*, as expected. Assays were performed in whole seedlings. Upper chart: total (PP2A + PP1), middle chart: PP2A, lower chart: PP1 activities. (b) Western blot analysis for the levels of PP2A/C in whole seedlings for controls of all genotypes involved in this study. This analysis shows that for the *fass* mutants, PP2A/C levels parallel their activities, while their level is decreased non-significantly in *c3c4* as compared to Col0. X = significant difference ($P < 0.05$), XX = significant difference ($P < 0.01$), XXX = significant difference ($P < 0.001$).

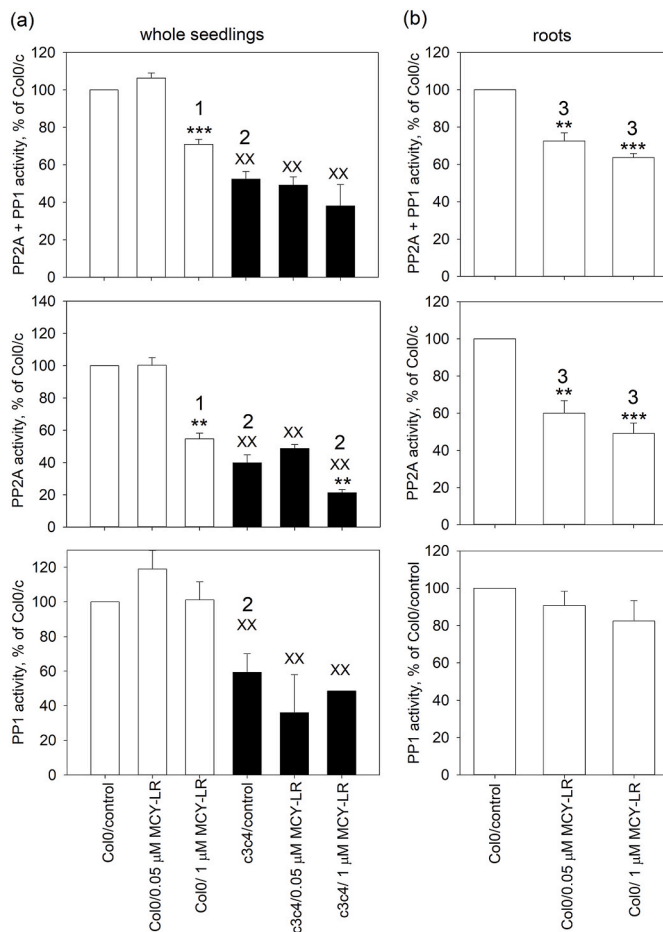


Fig. 2. Protein phosphatase activities in control and MCY-LR treated Arabidopsis genotypes-whole seedlings for Col0 and *c3c4* (a) and roots for Col0 (b). For more clarity, several significant issues are numbered on the graphs. Legends for numbers: 1- in whole plants of Col0, PP2A but not PP1 is inhibited by 1 μM MCY-LR; 2- in control *c3c4* whole plants, not only PP2A, but PP1 is also inhibited significantly and for PP2A, 1 μM , but not 0.05 μM MCY-LR induces further inhibition as compared to untreated *c3c4*; 3- in roots of Col0, both total PP2A + PP1 and PP2A activities are inhibited at the lower (0.05 μM) concentration of MCY-LR and at higher (1 μM) MCY concentration, inhibition is more pronounced. "X" symbols = significant differences between control wild-type (Col0) and control mutants, "***" symbols = significant differences between treatments within a given genotype. XX, ** = significant difference ($P < 0.01$), XXX, *** = significant difference ($P < 0.001$).

Col0 extracts examined (Fig. 2a, b/PP1 activity, lower graphs).

As stated before, for the *c3c4* mutant, total protein phosphatase, as well as both PP2A and PP1 activities were inhibited in controls (the mutants not treated with MCY-LR), while 0.05 μM MCY-LR did not cause any notable further inhibition. 1 μM MCY-LR induced further significant inhibition of PP2A (Fig. 2a/number 2 on graphs).

For the *fass* homozygote recessive (HZ) control (not treated with MCY-LR) whole seedlings, total phosphatase activities were higher as compared to Col0 as stated before (Figs. 1 and 3a, numbers 1 and 3 on upper graph for total activities). 0.05 μM MCY-LR did not induce significant changes in this activity pattern for *fass-5*, but inhibited PP2A activity significantly in *fass-15* (Fig. 3a, number 2, middle graph). 1 μM MCY-LR inhibited both PP2A and PP1 in both *fass* genotypes (Fig. 3/numbers 2 and 4 on graphs for MCY-LR treatments).

As concerning levels of PP2A/C (Western blot analysis) in whole seedlings not treated with MCY-LR, these subunits showed significant increases (as compared to Col0) in the *fass* mutants, while a non-significant decrease could be detected in *c3c4* (Fig. 1b). Extracts from

inhibitor treated seedlings of Col0 showed a significant decrease of PP2A/C levels at 0.05 μM MCY-LR, and 1 μM MCY-LR induced a slight/non-significant increase (Fig. 3b). Root protein extraction from Col0 for Western blot encountered protein stability problems, but our preliminary results indicate that MCY-LR had similar effects in Col0 roots as compared to whole seedlings (data not shown). In case of *fass-5* seedlings, inhibitor treatment did not induce significant changes (Fig. 3b), and preliminary results did not show significant changes for *fass-15* either as compared to the untreated plants of the respective genotype (data not shown).

3.2. Mitotic activities are affected in the *fass* and *c3c4* mutants and MCY-LR modulates mitosis in all genotypes

In case of controls (seedlings not treated with MCY-LR), mitotic activities of the RAM were similar for Col0 and *fass-15* HZs (Fig. 4). In contrast, mitosis was inhibited significantly in the *fass-5* HZs and *c3c4* (Fig. 4, upper graph). Moreover, arrests at early mitotic stages were observed for the *fass-5* HZ (Fig. 4, number 1 on the middle graph; compare early and late mitotic indices).

The effects of MCY-LR on mitotic activities were strongly genotype dependent. For Col0, this protein phosphatase inhibitory drug inhibited mitosis in a significant manner, but no mitotic arrest was observed (Fig. 5a). For *c3c4*, while controls showed decreased mitosis as compared to Col0, 0.05 μM MCY-LR increased mitotic index in a non-significant manner (Fig. 5a, number 1 on graph for early mitotic indices). 1 μM MCY-LR caused a slight further decrease of mitotic activity (Fig. 5a). For *fass-15*, there were no significant changes in terms of MCY-LR effects. Interestingly, in contrast to Col0, MCY-LR did not induce significant decreases of mitotic activities, however 0.05 μM MCY-LR induced arrests in late mitosis (Fig. 5b, number 2 on the lower graph for late mitotic indices). In case of *fass-5*, as stated before, HZ controls were characterized by decreased mitotic activities as compared to Col0. In addition, 0.05 μM MCY-LR induced an apparent increase of mitotic index, but this was due mainly to a more pronounced arrest in early mitosis as compared to *fass-5* HZ controls (Fig. 5b, middle graph/early mitotic indices, numbers 3 and 4 on graph). 1 μM MCY-LR caused a non-significant decrease in the percentage of cells in early mitosis (Fig. 5b, middle graph/early mitotic indices).

We were also looking for the occurrence of abnormal mitotic figures in all control and MCY-LR treated genotypes. As expected from literature data (e.g. Camilleri et al., 2002; Spinner et al., 2013), the *fass-5*, *fass-15* HZs and *c3c4* mutants did not develop preprophase MT bands (PPBs) at all. However, spindles were generally normal in both *fass* and *c3c4* mutants and were not affected notably by MCY-LR (data not shown).

3.3. The phosphorylation level of mitotic histone H3 in Col0 and mutants. Effects of MCY-LR

As expected, the immunohistochemical method employed here did not detect phospho-histone H3 (pH3-Ser10) in non-mitotic cells of the Arabidopsis RAM. In controls (no MCY-LR treatment) of Col0, the pH3-Ser10 phosphorylation pattern was as expected for mitotic plant cells (see e.g. Beyer et al., 2012). That is, pH3 was detected in mid-to late prophase, the fluorescence signal was the strongest in prometaphase and metaphase and declined in anaphase and early telophase. When phragmoplast was expanded and at cytokinesis, there was a total lack of signal (Fig. 6b and Suppl. Fig. S1). Besides studying the genotype and inhibitor dependent intensity of pH3-Ser10 signal, this labeling procedure was also helpful in more precise detection of mitotic phases. Prophase was difficult to detect solely by chromatin (DAPI) and microtubule (IHC) labeling (Suppl. Fig. S1/a). Because of the relatively small size of Arabidopsis chromosomes, even high-resolution DNA (DAPI) labeling images did not always reveal prophases clearly, while phospho-histone H3 labeling of pericentromeric chromosomal regions in mid-and late prophase were well detectable (Suppl. Fig. S1/b).

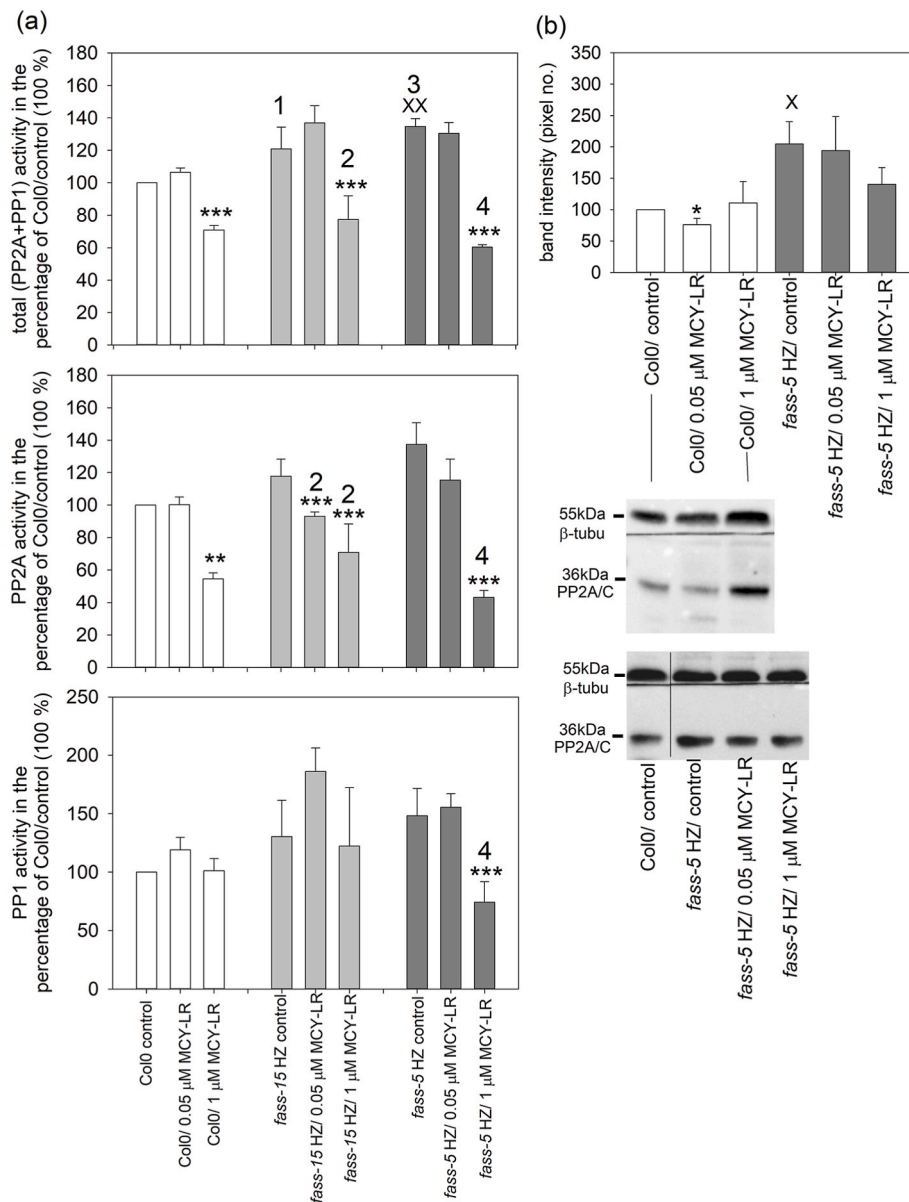


Fig. 3. (a) Protein phosphatase activities in control and MCY-LR treated Arabidopsis genotypes-whole seedlings of Col0 and *fass* homozygotes (HZs). For Col0, see Fig. 2 for explanation. For more clarity, several significant issues are numbered on the graphs. Legends for numbers: 1- in the *fass-15* homozygote controls (not treated with MCY-LR), both PP2A and PP1 activities are increased and 2- MCY-LR inhibits PP2A in a significant manner. 3- For *fass-5* homozygotes not treated with MCY-LR, both PP2A and PP1 activities are increased as compared to Col0, and as a result, total (PP2A + PP1) activities will increase in a significant manner; 4- however, in this genotype, 1 μ M MCY-LR induces a strong inhibition of both PP2A and PP1 activities. (b) Western blot analysis of PP2A/C levels in MCY-LR treated Col0 and *fass-5* whole seedlings. A significant decrease occurs in the presence of 0.05 μ M MCY-LR in Col0. "X" symbols = significant differences between control wild-type (Col0) and control mutants, "***" symbols = significant differences between treatments within a given genotype. X, * = significant difference ($P < 0.05$), XX, ** = significant difference ($P < 0.01$), *** = significant difference ($P < 0.001$).

For *c3c4*, pH3 levels were significantly higher than for Col0 in prophase and anaphase (Fig. 6a/compare black plot for Col0 to red plot, number 1 on graph; see also 6b for representative microscopy images). As concerning the *fass* mutants (HZs), *fass-15* was characterized by higher levels of pH3 in prophase and anaphase, but lower levels in prometaphase and metaphase (Fig. 6a/blue plot-squares). Major changes occurred in *fass-5*, where pH3 levels dropped significantly and dramatically (Fig. 6a/blue plot-inverted triangle, number 2 on graph; 6b). It is worth mentioning that 48 h after transfer of *fass-15* seedlings for treatments, this genotype has shown a drop of histone H3 phosphorylation, as for *fass-5* (to be published elsewhere).

MCY-LR induced several notable changes in pH3 levels in Col0 and *c3c4* as compared to the respective controls (Fig. 6c and d, number 3 on/

d/). In case of Col0, 1 μ M MCY-LR increased histone H3 phosphorylation during late mitosis (Fig. 6c). In case of *c3c4*, 0.05 μ M MCY-LR induced significant increases in nearly all mitotic phases (number 3 on Fig. 6d) and 1 μ M MCY-LR induced a significant increase during prophase (Fig. 6d). The inhibitor caused significant increases for HZs of *fass* as well. For *fass-15* HZs, 0.05 μ M MCY-LR left histone H3 phosphorylation unchanged except a drop at anaphase, while 1 μ M MCY-LR induced increases of pH3 levels at almost all phases of mitosis, with a significant and dramatic increase in metaphase (Fig. 6e). The most dramatic changes occurred for the *fass-5* HZs, where 0.05 μ M MCY-LR increased significantly pH3 levels that were almost restored to the levels of Col0 controls during early mitosis (Fig. 6f, number 4).

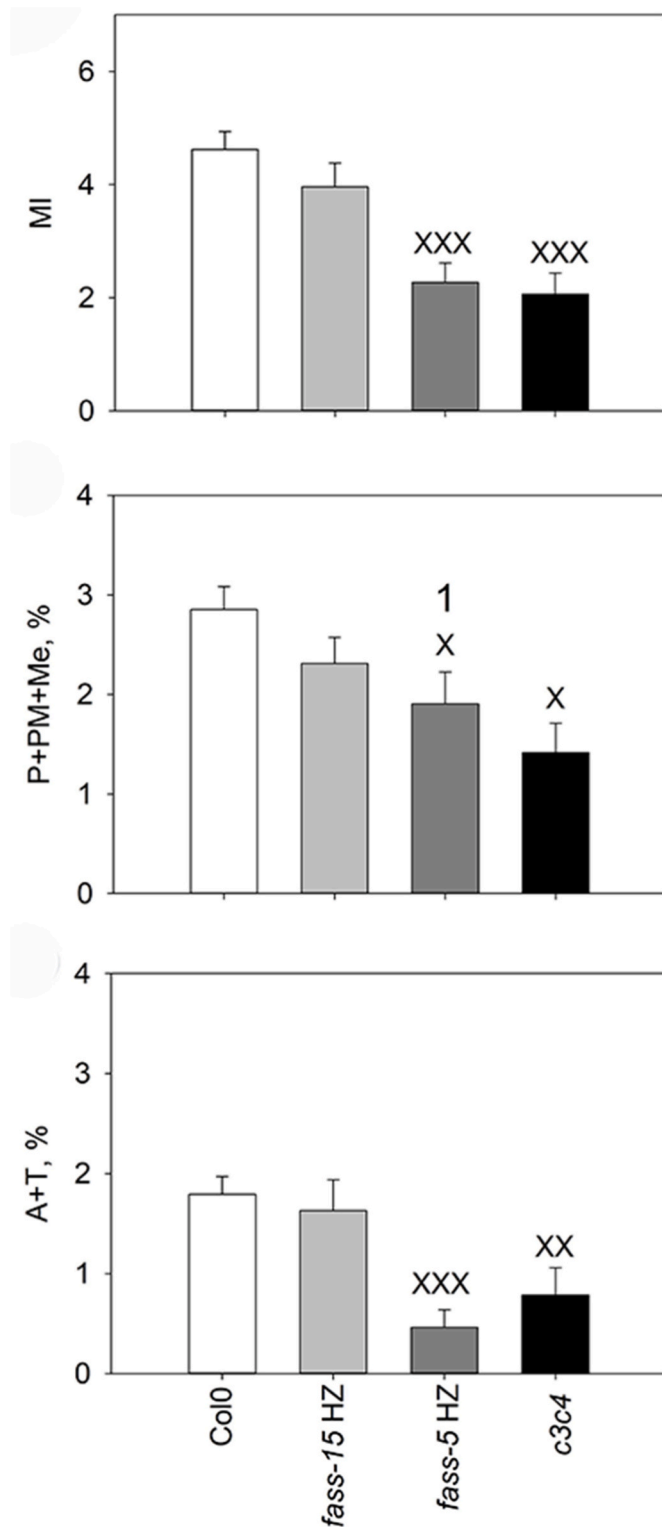


Fig. 4. Mitotic activities in the RAM of primary roots (not treated with MCY-LR) for all genotypes involved in this study as quantified from cells labeled with anti- β -tubulin, anti-pH3-Ser10 and DAPI. Labels on the y axes show mitotic index (MI, upper graph), percentage of cells in early mitosis (P + PM + Me, %, middle graph) and percentage of cells in late mitosis (A + T, %, lower graph). Upper graph shows low rates of mitosis in *fass-5* homozygote recessives and *c3c4*. For more clarity, several significant issues are numbered on the graphs. Number 1 on the middle graph indicates the block of cells in early mitosis in *fass-5* homozygote recessives. X = significant difference ($P < 0.05$), XX = significant difference ($P < 0.01$), XXX = significant difference ($P < 0.001$) between the wild-type RAM (Col0) and mutant.

4. Discussion

This work presents novel insights into the role of Fass in the modulation of PP2A/C activities and expression and the contribution of PP2A/C3-C4 subunits to overall catalytic activity. It was known previously, that Fass as a B'' subunit is involved in the regulation of PP2A holoenzyme localization to the cortical MTs and PPB (see Introduction section). There was a lack of knowledge on its related functions, e.g. how does it affect the activity of the PP2A catalytic subunits? To our surprise, for the *fass-5* and *fass-15* mutants (HZs), total PP2A + PP1 activities increased as compared to Col0 and both PP2A/C and PP1/C activities contributed to this. Total phosphatase activity increased in a significant manner in *fass-5* and Western blot analysis showed significant increases of total PP2A/C levels both in mutants showing weak (*fass-15*) and strong (*fass-5*) phenotypes (Fig. 1). Levels in the weaker phenotype are of more interest, making it more evident that these alterations are specific and not due to overall severe phenotypical alterations as in the strongly affected *fass-5* genotype. In general B regulatory subunits are known to regulate activity, substrate specificity and subcellular localization of the PP2A holoenzyme. For example B β subunit activates the PP2A holoenzyme to dephosphorylate EIR1 upon ethylene treatment in Arabidopsis (Máthé et al., 2023; Shao et al., 2022). We conclude that under normal conditions (wild-type Arabidopsis), Fass is a moderator of PP2A holoenzyme activity.

Fass interacts mainly with the C3 and C4 (class II) catalytic subunits of PP2A, and to a lesser extent, with the Class I C2 subunit as well (Yoon et al., 2018). We show here that the double *c3c4* mutants show severely decreased total phosphatase as well as PP2A/C and PP1/C activities. Meanwhile the levels of overall PP2A/C protein in this double mutant decrease (in a non-significant manner) as compared to Col0 (Fig. 1). Similarly, Yoon et al. (2018) detected decreases of total PP2A/C protein levels in Arabidopsis C-3,4 VIGS (virus-induced gene silencing system) plants. The low levels of full-length mRNA for C3 and the lack of full-length mRNA for C4 in the *c3c4* mutant (created by T-DNA insertions) (Spinner et al., 2013) predict that among catalytic subunits, C3 and C4 protein expression is low in the mutant and existing proteins are not functional. This means that the low PP2A activities and levels in this mutant detected in this study can be attributed to the lack of functional PP2A/C3 and PP2A/C4. Concerning the significant decrease of PP1 activity in *c3c4*, it is difficult to estimate whether this is a direct consequence of altered PP2A/C functionality or an indirect effect due to phenotypical and physiological alterations in the mutant (these alterations are shown e.g. in Freytag et al., 2023; Spinner et al., 2013). It is worth mentioning that diquat (DQ), an inducer of reactive oxygen species (not known to inhibit the protein phosphatases specifically) is also inhibiting PP1 activity in *c3c4* (Kelemen et al., 2024). These observations might indicate an indirect effect of these subunits on PP1. However, it should be noted that *c3c4*, as *fass-15*, is not as severely stunted as *fass-5*, for example it has offspring. Thus, we cannot exclude that C3 and C4 mediate a more direct interaction between PP2A and PP1, but this needs further evidence.

MCY-LR inhibits both PP2A and PP1 activities in vitro and in vivo for most of the organisms studied to date (MacKintosh and Diplexcito, 2010; Máthé et al., 2016). However, this study proves that for Arabidopsis Col0, only PP2A is inhibited in a significant manner by the drug in both roots and whole five days old seedlings at a relatively short (24h) treatment. Roots are more sensitive to the inhibitor: here, the lower MCY-LR concentration (0.05 μ M) does already inhibit overall PP2A/C activity, while for whole seedlings, only the higher inhibitor concentration (1 μ M) is effective (Fig. 2). Thus, MCY-LR is an excellent tool for the study of PP2A functions in Arabidopsis. It induces changes of auxin distribution (in Col0) or oxidative stress (in phosphatase related mutants) in Arabidopsis roots (Freytag et al., 2021, 2023): these alterations were related to its specific phosphatase inhibitory effects and were not only general stress reactions. The effects shown below are also attributed to its specific biochemical targets.

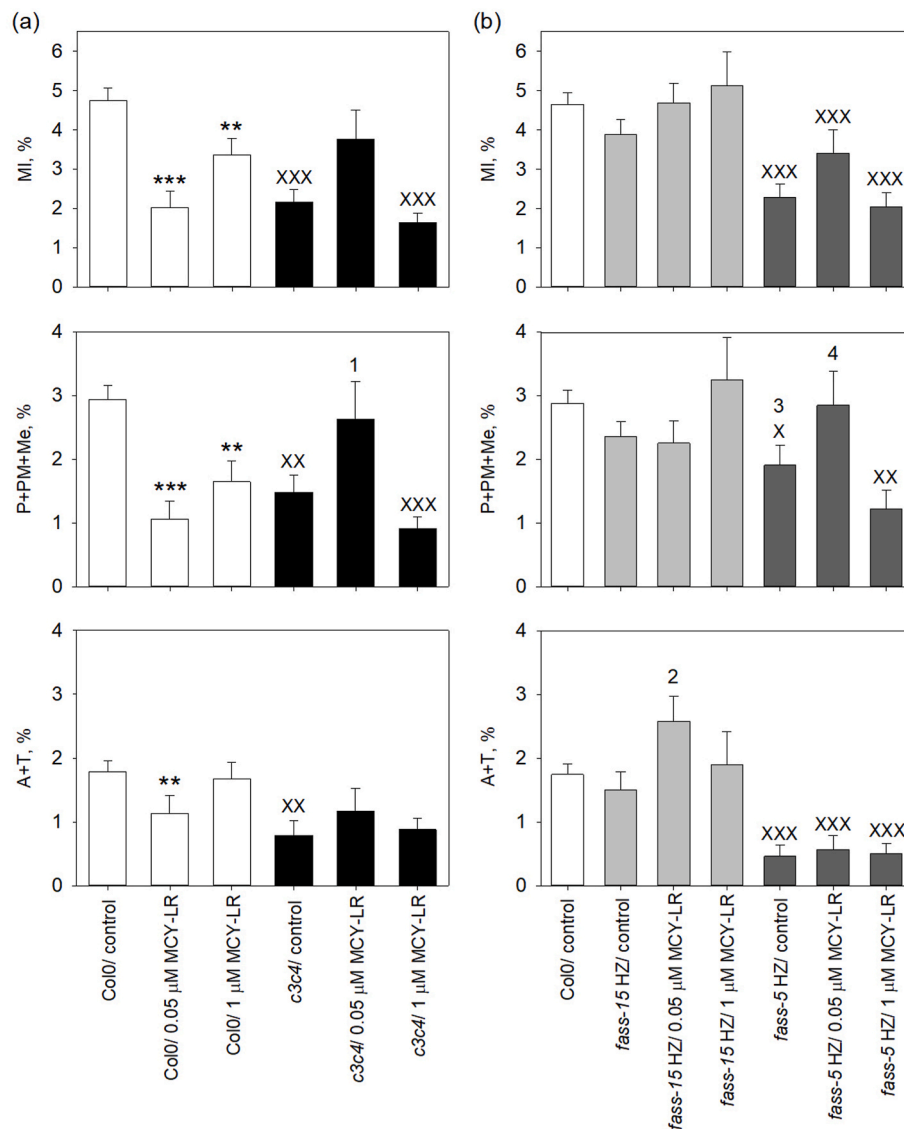


Fig. 5. Effects of MCY-LR on mitotic indices in Col0 and *c3c4* (a), *fass-15* and *fass-5* homozygotes (HZs) (b). For more clarity, several significant issues are numbered on the graphs. (a) shows that MCY-LR inhibits mitosis in Col0 (white bars) in a significant manner. Number 1 on the middle graph in (a) indicates a (non-significant) stimulation of mitosis at the treatment of *c3c4* roots with 0.05 μM MCY-LR. Number 2 on graph in (b)/late mitotic indices indicates blockages of cells in late mitosis in roots of *fass-15* homozygotes treated with 0.05 μM MCY-LR. Numbers 3 and 4 on graph in (b)/early mitotic indices indicate blockages in early mitosis in control and MCY-LR treated roots of *fass-5* homozygotes. “X” symbols = significant differences between control wild-type (Col0) and control mutants, “**” symbols = significant differences between treatments within a given genotype. X = significant difference ($P < 0.05$), XX, ** = significant difference ($P < 0.01$), XXX, *** = significant difference ($P < 0.001$).

MCY-LR has interesting effects on PP2A/C activities in mutants. In *c3c4*, 1 μM MCY-LR further decreases the already low activities (Fig. 2) indicating that the inhibitor is effective on the remaining functional PP2A/C subunits. For the *fass* mutants, MCY-LR inhibits PP2A both in the weak and strong alleles that show high phosphatase activities when untreated with the drug. This inhibition rate is nearly comparable to the inhibition of phosphatase activities in Col0 seedlings treated with 1 μM MCY-LR (Fig. 3). This indicates that the inhibitor is effective on overall PP2A functionality in the *fass* mutants as well. Interestingly, MCY-LR inhibits PP1 as well in *fass-5*. However, this mutant shows stronger phenotypic alterations, thus it is more sensitive to diverse stresses at the subcellular level as we demonstrated previously (Juhász et al., 2023)-therefore we may conclude that the alteration of PP1 activity (here, inhibition by MCY-LR) might not be related directly to the alteration of Foss-C3/C4 interaction.

How are the above modulations of protein phosphatase activities influencing mitotic parameters in the Arabidopsis RAM? According to

our previous studies on other model systems (Máthé et al., 2009; Beyer et al., 2012), we expected that phosphatase mutants and/or inhibitor treatments would show severe disruptions in the mitotic apparatus, inhibition and even blocking of mitosis. When the studied genotypes were not treated with MCY-LR, significant decreases of mitotic activities were detected in *fass-5* and *c3c4*. In *fass-5*, this was accompanied with the arrest of RAM cells in early mitotic phases (Fig. 4, number 1 on middle graph; Fig. 5b, number 3 on middle graph). Are these alterations related to specific effects of PP2A holoenzyme dysfunction or they are only consequences of the altered phenotypes of these mutants? Specificity for other alterations like those for mitotic microtubules in *fass* and *c3c4* has been shown in previous work (Spinner et al., 2013). *fass-15*, the less affected *fass* genotype does not show mitotic arrest symptoms for early mitosis, but shows a slight blockage in late mitosis in the presence of lower MCY-LR concentration (Fig. 5b, lower graph, number 2)- for the 5 + 1 days growth period used in this study. However, at further one day of growth (5 + 2 days), early mitotic arrest was observed in (MCY-LR

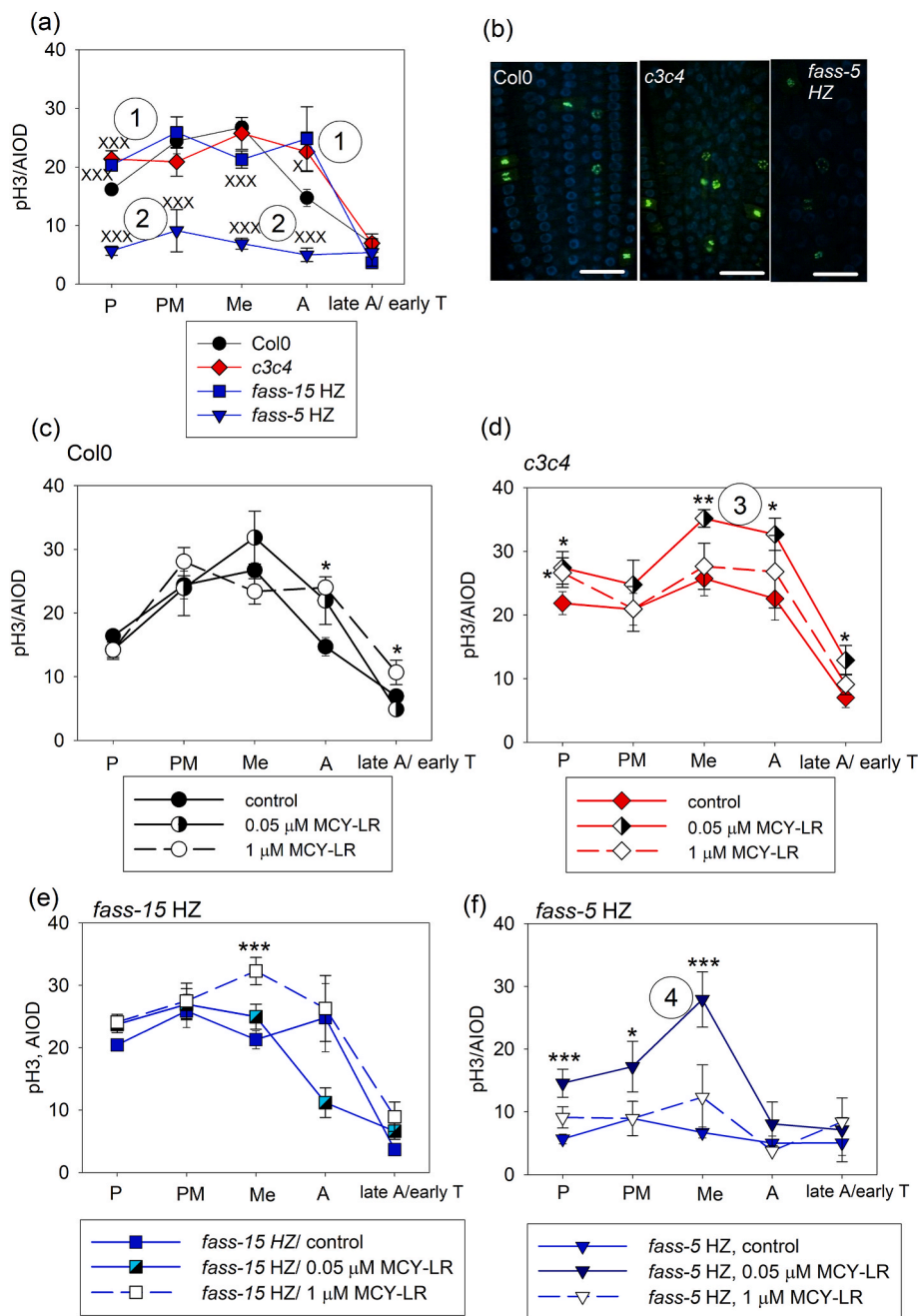


Fig. 6. Changes in the phosphorylation state of histone H3-Ser10 as shown by AIOD (area integrated optical density) data of Alexa488 signals from pH3-Ser10 labeling. (a) comparison of pH3-Ser10 levels in controls of all genotypes involved in this study. For more clarity, several significant issues are numbered on the graph. Number 1 indicates significantly higher pH3 levels in *c3c4* controls as compared to Col0 and number 2 indicates significantly lower pH3 levels in *fass-5* homozygotes, respectively. (b) representative images of pH3 immunolabeling (green signal of Alexa488 in the pale blue DAPI stained background) from control primary RAMs from Col0, *c3c4* and a *fass-5* homozygotes (HZs) to compare the intensities of histone H3 phosphorylation. Scalebars = 30 μ m. (c) Effects of MCY-LR on the progress of histone H3 phosphorylation in the Col0 RAM. (d) Effects of MCY-LR on the progress of histone H3 phosphorylation in the *c3c4* RAM. Number 3 indicates the significant elevations of pH3-Ser10 levels in the presence of 0.05 μ M MCY-LR. (e) Effects of MCY-LR on the progress of histone H3 phosphorylation in the RAM of *fass-15* homozygotes. 1 μ M MCY-LR increases the phosphorylation levels of H3 in metaphase. (f) Effects of MCY-LR on the progress of histone H3 phosphorylation in the RAM of *fass-5* homozygotes. As compared to the very low levels of histone H3 phosphorylation in controls, MCY-LR increases phosphorylation levels (number 4). X, * = significant difference ($P < 0.05$), ** = significant difference ($P < 0.01$), XXX, *** = significant difference ($P < 0.001$). (For interpretation of the references to colour in this figure legend, the reader is referred to the Web version of this article.)

treated *fass-15* as well (to be published elsewhere). We can conclude, that Fass regulates the onset of mitosis by keeping protein phosphatase activities and PP2A expression at normal levels-increases induced in PP2A + PP1 in the *fass* mutants induce mitotic arrest. Meanwhile, inhibition of mitosis in *c3c4* parallels the inhibition of phosphatase activities and decrease of PP2A levels without inducing mitotic arrest

(Fig. 1). In addition, it should be noted that all mutants studied here lack the formation of normal preprophase microtubule bands (PPBs) (Spinner et al., 2013). Because there is no early mitotic arrest in the *c3c4* RAM, we can assume that the lack of PPB does not inhibit transition from early to late mitosis in Arabidopsis and early mitotic arrest in *fass* is not related to PPB alterations. It is worth mentioning, that similarly to our

observations, Spinner et al. (2013) did not find mitotic arrest in the *c3c4* mutant. Overall, Fass may be involved in the regulation of the onset of mitosis, but this is not directly related to the regulation of PPB formation.

MCY-LR inhibits mitosis in parallel with the inhibition of PP2A in Col0 RAMs (compare Figs. 2 and 5a). Drug treated Col0 shows a direct relationship between PP2A and mitotic activities, a relation that seems to be a general feature of vascular plants. Interestingly, we showed that 0.05 μ M MCY-LR has a stronger inhibitory effect on mitosis, than 1 μ M MCY-LR, even though the higher inhibitor concentration has a stronger inhibitory effect on PP2A activities. Meanwhile, Western blots show that overall PP2A/C levels decrease at treatments with 0.05 μ M MCY-LR, but do not change significantly in the presence of 1 μ M MCY-LR. This might be caused by the perturbation of phosphatase activity-expression balance by the lower drug concentration, while the inhibitory effect at higher concentration might be compensated by maintaining normal PP2A levels (Fig. 3b and 5a). Previous studies for rice and cucumber seedlings show that as a compensatory mechanism, MCY-LR increases and not decreases phosphatase gene expression (Ma et al., 2023). Thus, the effects of the drug in terms of phosphatase expression might be plant species- and dose-dependent. Meanwhile, in *fass-5* (and *c3c4*), 0.05 μ M MCY-LR induces an apparent stimulation of mitosis as compared to untreated seedlings, but this is due mainly to an amplifying of early mitotic block in *fass-5* (but not in *c3c4*) (Fig. 5b, numbers 3–4). This effect is contrasting that observed in Col0 (inhibition of mitosis without mitotic block) but one should note that 0.05 μ M MCY-LR does not influence the expression of total PP2A/C protein in *fass-5* in contrast to the decrease of their levels in Col0 (Fig. 3b). For *fass-15*, we did not find inhibition of mitosis by MCY-LR, moreover, slight (although not significant) stimulatory effects can be detected (Fig. 5). These data give further support to the idea that the lack of functional Fass protein is inducing more complex effects, than merely influencing PP2A activities. Also, all these findings show that normal C3-C4 and Fass have specific effects in mitotic regulation partially distinct to general roles of PP2A holoenzymes. We suggest this needs thorough investigation and may be central to more detailed understanding of plant mitotic regulation.

MCY-LR, while inhibiting the total PP2A holoenzyme pool and increasing pH3Ser10 levels, does not arrest mitosis in Col0. It does have a blocking effect in *Vicia faba* (Beyer et al., 2012). Here, both PP2A and PP1 are inhibited by MCY-LR and in parallel, chromatin hypercondensation, histone H3 hyperphosphorylation and the inhibition of metaphase-anaphase transition can be observed (Beyer et al., 2012; Garda et al., 2018). Data on *V. faba* suggest that, both PP2A and PP1 as well as their complex relationships are involved in the proper phosphorylation state of histone H3 as well as of the onset and exit from mitosis. However, in Arabidopsis the phosphatase-mitosis-histone phosphorylation relationship is more complex. If a direct relationship would exist, we would expect that decreased PP2A activity induces histone H3 hyperphosphorylation and arrest in early mitosis, as in *V. faba* (Beyer et al., 2012; Garda et al., 2018). Obviously, increases of PP2A activities would induce contrary effects. Other previous studies have suggested that in plants, as for other eukaryotic cells, PP1 has a pivotal role in the dephosphorylation of histone H3, but raised the possibility for the role of PP2A as well (Beyer et al., 2012; Garda et al., 2018; Manzanero et al., 2002). Studies with protein phosphatase inhibitors may give evidence for this, but different PP2A inhibitors give diverse results (Beyer et al., 2012; Houben et al., 2007; Manzanero et al., 2002). However, the in vitro and in vivo (Arabidopsis) studies of Bíró et al. (2012) demonstrate that NAP-related proteins (nucleosome assembly proteins) inhibit PP2A activity and interact with both PP2A and pH3.

Among the Arabidopsis genotypes not treated with MCY-LR, *fass-5* shows severely altered (decreased) pH3-Ser10 levels (as compared to Col0 controls) after the 5 + 1 days growth period used in this study (Fig. 6a) and this is directly related to the increased PP2A/PP1 activities. The observed mitotic arrest contrasted our expectations, since low

pH3Ser10 would not induce this alteration. MCY-LR treated *fass-5* showed this alteration while increasing pH3Ser10 levels (compare Figs. 6f to 5b). However, decreased pH3 levels were found even in *fass-15* seedlings grown for an additional day (5 + 2 days, to be published elsewhere), but there was no mitotic arrest. The severe inhibition of both PP2A and PP1 in *c3c4* did induce increases in pH3-Ser10 levels in pro- and anaphase, but no significant mitotic arrests were observed (Fig. 6a, b, d). According to the above statements, we could find direct relationships between phosphatase activities and pH-Ser10 levels, but the mitotic arrest - histone H3 phosphorylation relationships in Arabidopsis are either lacking or they are more complex than expected.

Treatments with MCY-LR as a phosphatase inhibitor increased pH3-Ser10 levels in all the Arabidopsis genotypes studied (Fig. 6c–f), and for Col0, this is similar to our previous findings for *Vicia faba* RAMs (Beyer et al., 2012). However, in contrast to *V. faba* this was not related to mitotic arrest: for Col0, MCY-LR (even at the lower, 0.05 μ M concentration) inhibits mitotic activity and PP2A activities in roots, but does not induce arrests in early mitosis (Fig. 2a and 5a). For mutants, most notably in *c3c4* and *fass-5*, elevations of pH3Ser10 levels were more pronounced at MCY-LR treatments than in Col0 (Fig. 6c–f). This may indicate that dysfunctioning of these specific subunits will influence the related functioning of the general PP2A holoenzyme pool (MCY-LR inhibits all PP2A holoenzyme combinations). Interestingly in *fass-5*, 0.05 μ M MCY-LR restores pH3-Ser10 levels from very low to normal levels, while not changing significantly the activity and expression of PP2A/C protein (Figs. 3b and 6a, f). This is the single example, where we could not find a relationship between PP2A activity and pH3Ser10 levels.

To summarize histone H3 phosphorylation issues, while they depended on phosphatase activities, high pH3-Ser10 levels did not coincide with mitotic arrests in Arabidopsis in most of the cases/genotypes, regardless of the presence or absence of MCY-LR. This indicates that phosphatases regulate the above events in a different and more complex way in Arabidopsis vs. *Vicia*. Our results also suggest that lack of functional Fass protein may alter histone phosphorylation by inducing a mislocalization of the PP2A holoenzyme at the chromatin level. Overall, the regulation of mitotic exit is complex and many mechanisms need further investigation in Arabidopsis.

According to the above statements, we propose a model for the involvement of Fass/C3C4 in the regulation of PP2A activities in relation to mitotic events and histone H3 phosphorylation (Fig. 7). Therefore, the main conclusions of this study are.

- (i) Fass is regulating not only the correct subcellular localization of the PP2A holoenzyme, but it also keeps PP2A/C activity and expression at optimal levels. Its dysfunctioning raises and not decreases PP2A activities. PP2A/C3 and C4 contributes to the activities and levels of overall PP2A/C at optimal values.
- (ii) Fass and C3-C4 do regulate mitosis in Arabidopsis. PP2A in general and the subunits involved in this study in particular do play roles in histone H3 phosphorylation. The effects of MCY-LR on mitotic activities in Col0 and phosphatase mutants do also reveal the importance of overall PP2A functioning in the regulation of mitosis in general, in Arabidopsis. PP2A as a holoenzyme is partially involved in the direct regulation of metaphase-anaphase transition, but many other mechanisms are masking its function in Arabidopsis. Dysfunctioning of the C3-C4 catalytic subunits does not induce mitotic arrest. However, we have shown for the first time that Fass as a regulatory subunit may play more direct functions: mutants, especially *fass-5* do show mitotic arrest. However, this is not related directly to histone H3 phosphorylation in Arabidopsis.
- (iii) Fass and the interacting C3-C4 subunits are influencing PP1 activities. Currently we do not know the underlying biochemical mechanism. Due to the important functions of both PP2A and PP1 in plants, this needs much further investigation.

References

- Alonso, J.M., Stepanova, A.N., Leisse, T.J., Kim, C.J., Chen, H., Shinn, P., et al., 2003. Genome-wide insertional mutagenesis in *Arabidopsis thaliana*. *Science* 301, 653–657.
- Ballesteros, I., Domínguez, T., Sauer, M., Oaredes, P., Duprat, A., Rojo, E., Sanmartín, M., Sánchez-Serrano, J., 2013. Specialised functions of the PP2A subfamily II catalytic subunits PP2A-C3 and PP2A-C4 in the distribution of auxin fluxes and development in *Arabidopsis*. *Plant J.* 73, 862–872.
- Beyer, D., Tándor, I., Kónya, Z., Bátor, R., Roszik, J., Vereb, G., et al., 2012. Microcystin-LR, a protein phosphatase inhibitor, induces alterations in mitotic chromatin and microtubule organization leading to the formation of micronuclei in *Vicia faba*. *Ann. Bot.* 110, 797–808.
- Bheri, M., Pandey, G.K., 2019. PP2A phosphatases take a giant leap in the post-genomics era. *Curr. Genom.* 20, 154–171.
- Bíró, J., Farkas, I., Domoki, M., Ötvös, K., Bottka, S., Dombrádi, V., Fehér, A., 2012. The histone phosphatase inhibitory property of plant nucleosome assembly protein-related proteins (NRPs). *Plant Physiol. Biochem.* 52, 162–168.
- Bradford, M.M., 1976. A rapid and sensitive method for the quantitation of microgram quantities of protein utilizing the principle of protein-dye binding. *Anal. Biochem.* 72, 248–254.
- Camilleri, C., Azimzadeh, J., Pastuglia, M., Bellini, C., Grandjean, O., Bouchez, D., 2002. The *Arabidopsis* TONNEAU2 gene encodes a putative novel protein phosphatase 2A regulatory subunit essential for the control of the cortical cytoskeleton. *Plant Cell* 14, 833–845.
- Dedinszki, D., Sipos, A., Kiss, A., Bátor, R., Kónya, Z., Virág, L., et al., 2015. Protein phosphatase-1 is involved in the maintenance of normal homeostasis and in UVA irradiation-induced pathological alterations in HaCaT cells and in mouse skin. *Biochim. Biophys. Acta (BBA) - Mol. Basis Dis.* 1852, 22–33.
- Demidov, D., Van Damme, D., Geelen, D., Blattner, F.R., Houben, A., 2005. Identification and dynamics of two classes of Aurora-like kinases in *Arabidopsis* and other plants. *Plant Cell* 17, 836–848.
- Erdődi, F., Tóth, B., Hirano, K., Hirano, M., Hartshorne, D.J., Gergely, P., 1995. Endothal thioanhydride inhibits protein phosphatases-1 and -2A in vivo. *Am. J. Physiol.* 269, C1176–C1184.
- Farkas, I., Dombrádi, V., Miskei, M., Szabados, L., Koncz, C., 2007. *Arabidopsis* PPP family of serine/threonine phosphatases. *Trends Plant Sci.* 12, 169–176.
- Freytag, C., Máthé, C., Rigó, G., Nodzyński, T., Kónya, Z., Erdődi, F., et al., 2021. Microcystin-LR, a cyanobacterial toxin affects root development by changing levels of PIN proteins and auxin response in *Arabidopsis* roots. *Chemosphere* 276, 1–10.
- Freytag, C., Garda, T., Kónya, Z., M-Hamvas, M., Tóth-Várady, B., Juhász, G.P., et al., 2023. B⁺ and C subunits of PP2A regulate the levels of reactive oxygen species and superoxide dismutase activities in *Arabidopsis*. *Plant Physiol. Biochem.* 195, 182–192.
- Gamborg, O.L., Miller, R.A., Ojima, K., 1968. Nutrient requirements of suspension cultures of soybean root cells. *Exp. Cell Res.* 50, 151–158.
- Garda, T., Kónya, Z., Freytag, C., Erdődi, F., Gonda, S., Vasas, G., et al., 2018. Allyl-isothiocyanate and microcystin-LR reveal the protein phosphatase mediated regulation of metaphase-anaphase transition in *Vicia faba*. *Front. Plant Sci.* 9, 1–15.
- Houben, A., Demidov, D., Caperta, A.D., Karimi, R., Agueci, F., Vlasenko, L., 2007. Phosphorylation of histone H3 in plants - a dynamic affair. *Biochim. Biophys. Acta* 1769, 308–315.
- Juhász, G., Kéki, S., Dékány-Adamoczy, A., Freytag, C., Vasas, G., Máthé, C., Garda, T., 2023. Microcystin-LR, a cyanobacterial toxin, induces changes in the organization of membrane compartments in *Arabidopsis*. *Microorganisms* 11, 1–13.
- Kelemen, A., Garda, T., Kónya, Z., Erdődi, F., Ujlaky-Nagy, L., Juhász, G.P., et al., 2024. Treatments with diquat reveal the relationship between protein phosphatases (PP2A) and oxidative stress in *Arabidopsis thaliana* root meristems. *Plants* 13, 1896.
- Kirik, A., Ehrhardt, D., Kirik, V., 2012. TONNEAU/FASS regulates the geometry of microtubule nucleation and cortical array organization in interphase *Arabidopsis* cells. *Plant Cell* 24, 1158–1170.
- Kós, P., Gorzó, G., Surányi, G., Borbely, G., 1995. Simple and efficient method for isolation and measurement of cyanobacterial hepatotoxins by plant tests (*Sinapis Alba* L.). *Anal. Biochem.* 225, 49–53.
- Laemmli, U.K., 1970. Cleavage of structural proteins during assembly of the head of bacteriophage T4. *Nature* 227, 680–685.
- Linkert, M., Rueden, C.T., Allan, C., Burel, J.-M., Moore, W., Patterson, A., et al., 2010. Metadata matters: access to image data in the real world. *JCB (J. Cell Biol.)* 189, 777–782.
- Ma, X., Gu, Y., Liang, C.K., 2023. Adaptation of protein phosphatases in *Oryza sativa* and *Cucumis sativus* to microcystins. *Environ. Sci. Pollut. Res.* 30, 7018–7029.
- MacKintosh, C., Diplecixto, J., 2010. Chapter 87 - naturally occurring inhibitors of protein serine/threonine phosphatases. In: Bradshaw, R.A., Dennis, E.A. (Eds.), *Handbook of Cell Signaling*, second ed. Elsevier, pp. 683–687.
- Manzanero, S., Rutten, T., Kotseruba, V., Houben, A., 2002. Alterations in the distribution of histone H3 phosphorylation in mitotic plant chromosomes in response to cold treatment and the protein phosphatase inhibitor cantharidin. *Chromosome Res.* 10, 467–476.
- Máthé, C., Beyer, D., Erdődi, F., Serfőző, Z., Székvölgyi, L., Vasas, G., et al., 2009. Microcystin-LR induces abnormal root development by altering microtubule organization in tissue-cultured common reed (*Phragmites australis*) plantlets. *Aquat. Toxicol.* 92, 122–130.
- Máthé, C., Beyer, D., Mikóné Hamvas, M., Vasas, G., 2016. The effects of microcystins (cyanobacterial heptapeptides) on the eukaryotic cytoskeletal system. *Mini Rev. Med. Chem.* 16, 1063–1077.
- Máthé, C., M-Hamvas, M., Vasas, G., Garda, T., Freytag, C., 2021. Subcellular alterations induced by cyanotoxins in vascular plants - a review. *Plants* 10, 984.
- Máthé, C., Freytag, C., Kelemen, A., M-Hamvas, M., Garda, T., 2023. “B⁺” regulatory subunits of PP2A: their roles in plant development and stress responses. *Int. J. Mol. Sci.* 24, 5147.
- Motta, M.R., Schnitger, A., 2021. A microtubule perspective on plant cell division. *Curr. Biol.* 31, R496–R552.
- Murashige, T., Skoog, F., 1962. A revised medium for rapid growth and bio assays with tobacco tissue cultures. *Physiol. Plantarum* 15, 473–497.
- Nagy, M., Kéki, S., Rácz, D., Mathur, J., Vereb, G., Garda, T., et al., 2018. Novel fluorochromes label tonoplast in living plant cells and reveal changes in vacuolar organization after treatment with protein phosphatase inhibitors. *Protoplasma* 255, 829–839.
- Pasternak, T., Tietz, O., Rapp, K., Begheldo, M., Nitschke, R., Ruperti, B., et al., 2015. Protocol: an improved and universal procedure for whole-mount immunolocalization in plants. *Plant Methods* 11, 50.
- Rasmussen, C.G., Bellinger, M., 2018. An overview of plant division-plane orientation. *New Phytol.* 219, 505–512.
- Schaefer, E., Belcram, K., Uyttewaal, M., Duroc, Y., Goussot, M., Legland, D., et al., 2017. The preprophase band of microtubules controls the robustness of division orientation in plants. *Science* 356, 186–189.
- Schindelin, J., Arganda-Carreras, I., Frise, E., Kaynig, V., Longair, M., Pietzsch, T., et al., 2012. Fiji: an open-source platform for biological-image analysis. *Nat. Methods* 9, 676–682.
- Shao, Z., Zhao, B., Kotla, P., Burns, J.G., Tran, J., Ke, M., et al., 2022. Phosphorylation status of B⁺ subunit acts as a switch to regulate the function of phosphatase PP2A in ethylene-mediated root growth inhibition. *New Phytol.* 236, 1762–1778.
- Shi, Y., 2009. Serine/Threonine phosphatases: mechanism through structure. *Cell* 139, 468–484.
- Spinner, L., Gadeyne, A., Belcram, K., Goussot, M., Moison, M., Duroc, Y., et al., 2013. A protein phosphatase 2A complex spatially controls plant cell division. *Nat. Commun.* 4, 1863.
- Vasas, G., Gáspár, A., Páger, C., Surányi, G., Máthé, C., Hamvas, M.M., et al., 2004. Analysis of cyanobacterial toxins (anatoxin-a, cylindrospermopsin, microcystin-LR) by capillary electrophoresis. *Electrophoresis* 25, 108–115.
- Virshup, D.M., Shenolikar, S., 2009. From promiscuity to precision: protein phosphatases get a makeover. *Mol. Cell* 33, 537–545.
- Waadt, R., Schmidt, L.K., Lohse, M., Hashimoto, K., Bock, R., Kudla, J., 2008. Multicolor bimolecular fluorescence complementation reveals simultaneous formation of alternative CBL/CIPK complexes in planta. *Plant J.* 56, 505–516.
- Yoon, J.T., Ahn, H.K., Pai, H.S., 2018. The subfamily II catalytic subunits of protein phosphatase 2A (PP2A) are involved in cortical microtubule organization. *Planta* 248, 1551–1567.